Acute Effects of Intraocular Pressure-Induced Changes in Schlemm's Canal Morphology on Outflow Facility in Healthy Human Eyes

Wei Chen, Tian Hu, Qiongfang Xu, Zhiqi Chen, Hong Zhang, and Junming Wang

Department of Ophthalmology, Tongji Hospital, Tongji Medical College, Huazhong University of Science and Technology, Wuhan, China

Correspondence: Junming Wang, Department of Ophthalmology, Tongji Hospital, Tongji Medical College, Huazhong University of Science and Technology, Wuhan 430030, China; eyedrwjm@163.com.

WC and TH contributed equally.

Received: March 12, 2020
Accepted: June 16, 2020
Published: July 27, 2020

Citation: Chen W, Hu T, Xu Q, Chen Z, Zhang H, Wang J. Acute effects of intraocular pressure-induced changes in schlemm's canal morphology on outflow facility in healthy human eyes. *Invest Ophthalmol Vis Sci.* 2020;61(8):36. https://doi.org/10.1167/iovs.61.8.36

Purpose. To estimate the outflow facility coefficient (C) as a function of Schlemm's canal cross-sectional area (SCAR) in healthy subjects using noninvasive oculopression tonometry (OPT).

Methods. In 25 healthy volunteers, intraocular pressure (IOP) decay values were recorded by a ophthalmodynamometer, with a fixed external force (0.15 N) on the inferior-temporal eyelid, every 10 seconds, for four minutes, and again after a 30-minute rest. Schlemm's canal profile images and IOP were obtained pre-procedurally (baseline), immediately (T0), and at 1-minute intervals post-procedurally (T1, T2, T3, and T4). C was calculated for different IOPs. The SCAR, coronal, and the meridional diameter of Schlemm's canal were calculated.

Results. Mean C_0 for the maximum IOP was 0.020 ± 0.017 µL/min/mm Hg; mean C was 0.018 ± 0.0071 and 0.058 ± 0.0146 µL/min/mm Hg at 40 and 20 mm Hg, respectively. C was nonlinearly dependent on the IOP (R^2 = 0.945). The SCAR was 5440 ± 3140.82, 3947.6 ± 2246.8, and 5375.7 ± 2662.7 µm^2 at baseline, T0, and T4, respectively. The coronal diameter of SC decreased significantly from the baseline (33.02 ± 11.3 µm) to T0 (26.6 ± 9.37 µm) and recovered at T4 (32.3 ± 9.53 µm). The SCAR and IOP correlated significantly throughout (R^2 = 0.9944; P < 0.001). C0 significantly correlated with the SCAR at baseline and with changes in the SCAR and IOP from T0 to T4.

Conclusions. Schlemm's canal dimensions are responsible for the IOP-dependent mechanical forces, and these changes appear to directly affect outflow facility.

Keywords: Schlemm's canal, aqueous humor outflow, optic coherence tomography, oculo-pression tonometry

Aqueous humor is formed by the ciliary processes and exits the eye mainly at the anterior chamber angle. Intraocular pressure (IOP) is determined by the dynamic equilibrium of the aqueous humour formation and outflow through the conventional outflow pathway or the unconventional route.[1] The resistance to aqueous humor outflow through the conventional path is usually expressed by the outflow facility coefficient (C, mL/min/mm Hg). Impairment of the conventional outflow pathway leads to a decrease in the outflow facility and an increase in IOP, which is the major risk factor for progression of glaucoma.[2]

Although outflow facility measurement is not adopted in routine clinical practice, it is an important research tool for revealing the physiological properties of the eye and the different mechanisms of antiglaucoma medications and surgeries.[3,4] Electronic Schitøz tonometry[5] and pneumatonography[6] have been used to measure the outflow facility in numerous studies. Outflow facility was calculated from the pressure decay curves, and then the C value was estimated using the Langham's pressure-volume relationship tables and a polynomial fitted to the decay curve. Although it has been verified that a decreased outflow facility causes IOP elevation in most types of glaucoma, the factors controlling the outflow facility remain largely unknown.[7]

Earlier laboratory research has shown that the primary site of conventional outflow resistance mainly involves the trabecular meshwork and the inner wall region of the Schlemm's canal (SC),[8] but depending on the traditional methods used (electronic Schitøz tonometry or pneumatonography), the pathophysiological changes (the configuration of anterior chamber angle, the morphology of SC, and trabecular meshwork [TM]) in the outflow pathway cannot be observed that coincide with changes in the outflow resistance. Thus the mechanism and precise location of the outflow resistance of the aqueous humour remains unclear. In this study, we estimated the outflow facility coefficient (C) as a function of the cross-sectional area of SC (SCAR), using noninvasive oculo-pression tonometry (OPT) to gain insight into the mechanism underlying the outflow resistance.

Methods

Ethics Statement

The study protocols were approved by the ethics committee of Tongji Hospital and registered with the Chinese clinical trials registry (ChiCTR-ROC-16008832). Written informed consent was obtained before enrollment from all the participants, in accordance with the tenets set forth in the Declaration of Helsinki.

Study Subjects

Twenty-five healthy volunteers from Tongji Hospital in Wuhan (Hubei Province, China) were recruited between June 2019 and October 2019. A single eye was enrolled randomly for all subjects.

Inclusion criteria were as follows: (1) IOP < 21 mm Hg and normal ophthalmoscopic appearance of the optic nerve (cup-to-disc ratio < 0.5 in both eyes, cup-to-disc ratio asymmetry < 0.2, absence of hemorrhage, and localized or diffuse rim thinning); (2) age > 18 years; and (3) no history of use of medication that affects the circulatory system within the month before enrollment.

Exclusion criteria were as follows: (1) Best-corrected visual acuity < 20/20; (2) refractive error (RE) ≤ −6.0 D and RE ≥ +3.0 D; (3) presence of other eye diseases such as age-related macular degeneration, retinal detachment, or a history of previous eye operations; and (4) history of or current hypertension or diabetes or familial history of these conditions.

Acute Transient Elevation of Intraocular Pressure Measurement

IOP was measured in the sitting position by using an I-care rebound tonometer (I-Care Finland Oy, Vantaa, Finland). The ophthalmodynamometer (Luneau L150, Luneau Technology, Pont-de-l'Arche, France) was used to apply external pressure on the eyeball through the temporal lower lid, with the device held perpendicular to the globe. According to the ophthalmodynamometer scale, the external force applied (0.15 N) increased the IOP by a fixed amount. One experimenter (H.T.) kept the ophthalmodynamometer steady in place while another experimenter (C.W.) measured and read the IOP readings (every 10 seconds for 4 minutes) and the third experimenter (Q.F.X.) recorded the data (the timepoints and the IOP readings).

Outflow Facility Coefficient Calculation

When the external force (0.15 N) reached the set pressure reading on the ophthalmodynamometer scale, the maximum IOP was achieved and the IOP one-phase decay curve over time was recorded for 4 minutes (Fig. 1). The outflow facility coefficient C can be calculated from the experimental data as follows:[9]

$$C = \frac{\frac{dP}{dt_1} \cdot \frac{1}{KP_1} - \frac{dP}{dt_2} \cdot \frac{1}{KP_2}}{P_2 - P_1}, \quad (1)$$

where P_1 and P_2 correspond to different IOP recordings. K is the ocular rigidity coefficient, and C is the outflow facility coefficient.

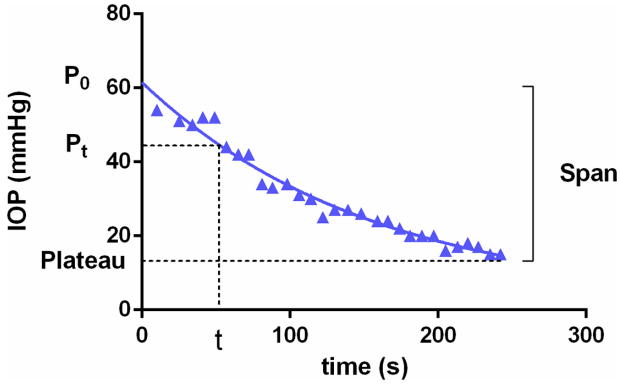

Figure 1. IOP decay curve over time. The *blue triangles* are the IOPs at specific times.

The pressure data recorded during the outflow measurement were filtered using an exponential custom fit for each subject, using the following equation:

$$f'(t) = P_{plateau} + P_{span} \times exp^{-at}, \quad (2)$$

where $f'(t)$ corresponds to the rate constant in units that are the derivative of the X-axis units. P equals P_0 at $t = t_0$, then decays down to a plateau in one phase.

Schlemm's Canal and Trabecular Meshwork

After the four-minute IOP recording, a 30-minute rest period was provided. Then, the IOP and anterior segmental image were captured (baseline). Subsequently, the external force was again applied to the eyeball through the temporal lower lid, using a fixed amount (0.15 N) for four minutes. An anterior segmental image and IOP were obtained immediately (T0) and sequentially for four times, every one minute (T1, T2, T3, and T4).

Rectangle scans were used to assess the nasal regions of the selected eye of each subject by using the anterior segment module of the Spectralis optical coherence tomography (OCT) scanner (EDI-OCT; Spectralis; Heidelberg Engineering GmbH, Dossenheim, Germany). For a rectangular area of 15 × 5°, 21 serial EDI-OCT B-scans were obtained (20 frames were stacked to generate one EDI OCT B-scan). All OCT tests were performed under standardized darkroom photopic conditions (ca. 3.5 lux).

Conjunctival vessels and iris crypts were used as landmarks to scan the same limbal area. The SCAR (μm²), the coronal diameter of SC (μm), the meridional diameter of SC (μm), nasal trabecular iris angle at 500 μm (TIA500°), and trabecular meshwork thickness (μm) were measured using the Image J software (version 1.45 S; National Institutes of Health, Bethesda, MD, USA) (Figs. 2A–2C).[10–12] The measurements were performed by two observers (W.C, T.H); cases of discrepancy >15% were resolved by consulting the senior author (J.M.W). The data were recorded and stored for later statistical analysis.

Statistical Analysis

All statistical analyses were performed using SPSS software (Version 16.0; SPSS Inc., Chicago, IL, USA). The data are presented as mean values ± standard deviations

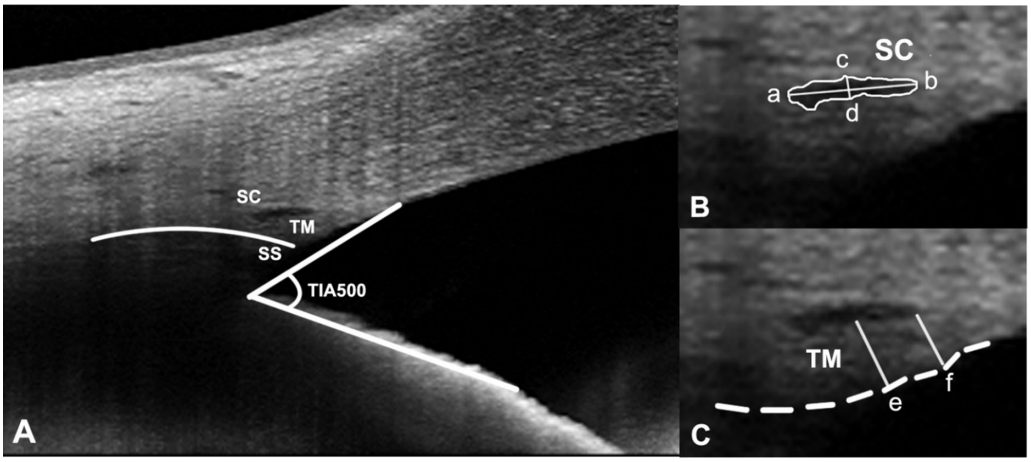

Figure 2. **A,** Anterior chamber angle image. SS, scleral spur; TIA500, trabecular iris angle (Apex in the iris sulcus and arms passing through the point 500 µm from SS and the point perpendicularly opposite on the iris). **B,** The *white circle* represents the SC lumen. *a–b line*: the meridional diameter of SC; *c–d line*: the coronal diameter of SC. **C,** The *dotted line* shows the meshwork inner layer and trabecular meshwork thickness calculated by the mean values of the perpendicular distance of *e and f lines* from the SC inner wall to the meshwork inner layer. The *e-line* is at the midpoint of the SC cross-sectional opening, and *d-line* made at the anterior endpoint of SC.

Table 1. Baseline Characteristics

Parameters	Values
Number of subjects	25
Number of eyes	25
Age (year)	25.04 ± 1.27
Sex (number of individuals studied)	
Female	14
Male	11
IOP (mm Hg)	16.8 ± 2.5
Refractive error (diopter)	−2.3 ± 1.5
Central cornea thickness (µm)	550 ± 13.6

Table 2. Measuring of Outflow Facility Coefficient in Different IOP Levels

IOP (mm Hg)	C Value (µL/min/mm Hg)
40 mm Hg	0.018 ± 0.0071
35 mm Hg	0.019 ± 0.0062
30 mm Hg	0.021 ± 0.0086
25 mm Hg	0.023 ± 0.0108
20 mm Hg	0.058 ± 0.0146

Data are presented as mean ± standard deviation.

(means ± SDs). One-way repeated-measures analysis of variance was used to compare variations in the SCAR, the coronal and meridional of SC, IOP, TIA500, and thickness of the trabecular meshwork (TMTH) at different time-periods (baseline and every one minute for four minutes). Linear regression analyses were adopted to examine the relationship between the C value and SCAR at baseline, the differences in SCAR at maximum IOP and baseline (ΔSCAR), baseline IOP, and the differences in IOP between maximum and baseline (ΔIOP). All tests were two-tailed. Statistical significance was defined as a P-value < 0.05.

Results

Twenty-five eyes from 25 healthy subjects (11 males and 14 females), aged 24–27 years (25.04 ± 1.27 years) were included in the study. The mean axial length was 24.24 ± 0.80 mm, and the mean baseline IOP was 16.8 ± 2.5 mm Hg before the procedure, as determined with the I-care (Table 1). The value of C_0 (C_0 corresponding to the initial maximum IOP) of all subjects was 0.020 ± 0.017. There was a significant inverse dependency of the C value on the IOP level (exponential one-phase decay curve; $R^2 = 0.945$) (Fig. 3), which was evident in all subjects. The average C value for the IOP was 0.018 ± 0.0071 µL/min/mm Hg at 40 mm Hg, which increased to an average of 0.058 ± 0.0146 µL/min/mm Hg at 20 mm Hg (Table 2).

The SCAR was 5440.0 ± 3140.8 µm^2 at 16.8 mm Hg at baseline, which decreased to 3947.6 ± 2246.8 µm^2 at 38.6 mm Hg at T0, then returned to 5375.7 ± 2662.7 µm^2 at 14.4 mm Hg at T_4 (Fig. 4). The SCAR correlated significantly with the IOP levels from baseline to T4 ($R^2 = 0.9944$; $P < 0.001$ (Figs. 5A, 5B).

The coronal diameter of SC decreased significantly from 33.02 ± 11.3 µm at baseline to 26.6 ± 9.37 µm at T0 and returned to 32.3 ± 9.53 µm at T4. The meridional diameter of SC decreased significantly from 259.4 ± 90.0 µm at baseline to 251.2 ± 91 µm at T0 and returned to 258.7 ± 73.5 µm at T4. There were no significant differences in trabecular meshwork thickness and TIA-500 at any different timepoints (Figs. 5C, 5D).

There was a significant correlation between the C_0 and the SCAR and IOP at baseline. At four minutes, after applying a stable external force, C_0 correlated with the differences in SCAR and IOP between T0 and T4 (ΔSCAR and ΔIOP, respectively; Figs. 6A–6D).

Discussion

Ocular pression tonometry (OPT) was first applied by Ulrich in 1987,[14] in glaucoma patients, to assess the outflow facility in a manner similar to the tonography performed. Ocular parameters can be measured simultaneously in the process of OPT. Because the OPT is easier to perform and is better tolerated than the standard tonography techniques, it has been widely adopted in recent years.[15–19]

Investigative Ophthalmology & Visual Science

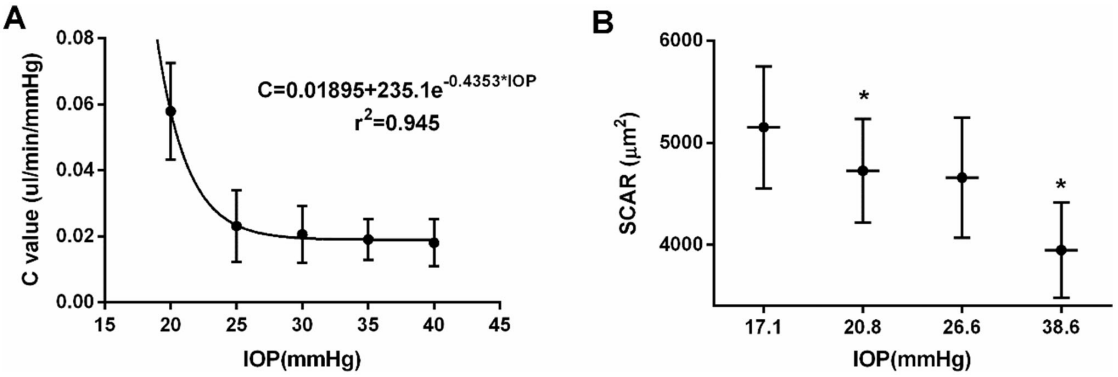

Figure 3. **A**, There was a significant nonlinear dependency of the C value on the IOP levels (Exponential one-phase decay curve). C value continuously declined with an IOP above 20 mm Hg. **B**, SCAR was found decreased, as expected, by the increased IOP. *Asterisk* denotes statistically significant differences (one-way repeated-measures analysis of variance, $P < 0.05$).

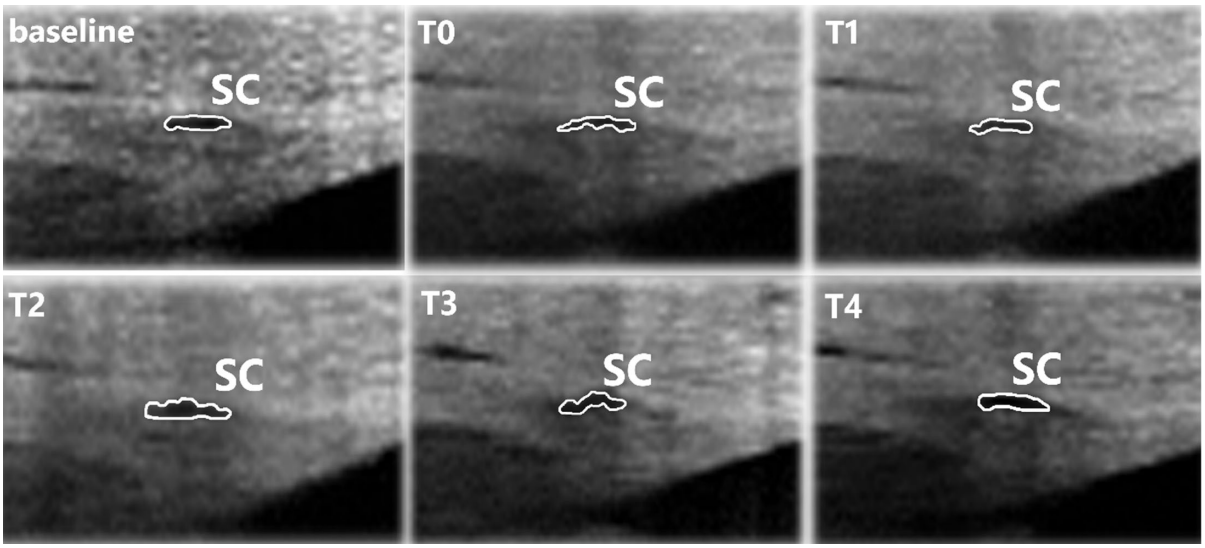

Figure 4. The anterior chamber angle images were obtained during different time-points of the study. SC lumen appeared collapsed at T0 and gradually returned at T4, both of which were compared to the image at baseline. The *white circle* depicts the SC lumen. Time points: An anterior segmental image was obtained before (baseline), immediately (T0), and sequentially, four times, every 1 minute (T1, T2, T3, and T4).

In this study, the outflow facility coefficient (C) was influenced by the balance of IOP and outflow steady rate, which reflects the resistance to the aqueous humor outflow. Using OPT in vivo in healthy human eyes, we demonstrated that morphology changes in the SC and outflow facility are significantly linked and that, when the IOP exceeds 20 mm Hg, the outflow facility starts to decline markedly.

SC has attracted considerable interest in recent years, due to the unique microstructure of the endothelial cells in the inner wall and its potential function in keeping IOP stable.[20,21] The aqueous humor flows through the conventional pathway, comprised of the trabecular meshwork and SC, and drains into the collecting channels and aqueous veins. Outflow resistance is mainly generated near SC, but the precise location and mechanism by which this dissipation occurs, remain a matter of contention. Some investigators have proposed that the resistance arises in the juxtacanalicular connective tissue (JCT) in particular, because of the abundant extracellular matrix and collagens.[22] However, the hydraulic conductivity, which reflects the flow resistance across the connective tissue, is extremely low in the JCT (about 65×10^{-14} cm^2 as calculated by porous media theory[23] and $2000–10{,}000 \times 10^{-14}$ cm^2 based on photomicrographs[24]). Accordingly, numerous investigators have concluded that the JCT would generate an insignificant fraction of outflow resistance.[23–26] The pores and giant vacuoles of the endothelium of the SC are also thought to modulate the aqueous humor outflow resistance.[27] In morphologic studies, mathematical modeling revealed that the dilation of SC led to an increased outflow facility.[28,29] By using a morphometric analysis system, Allingham et al.[30] found that the reduction in SC dimensions in eyes with primary open-angle glaucoma may account for approximately half of the decrease in the outflow facility. In our study, after the acute IOP elevation, there was a significant decrease in the SCAR, which was accompanied by a decrease in the outflow facility in the healthy subjects; however, the thickness of the trabecular meshwork remained unchanged. Changes in the SCAR from 0 to 4 minutes after the external pressure elevation, correlated significantly and positively

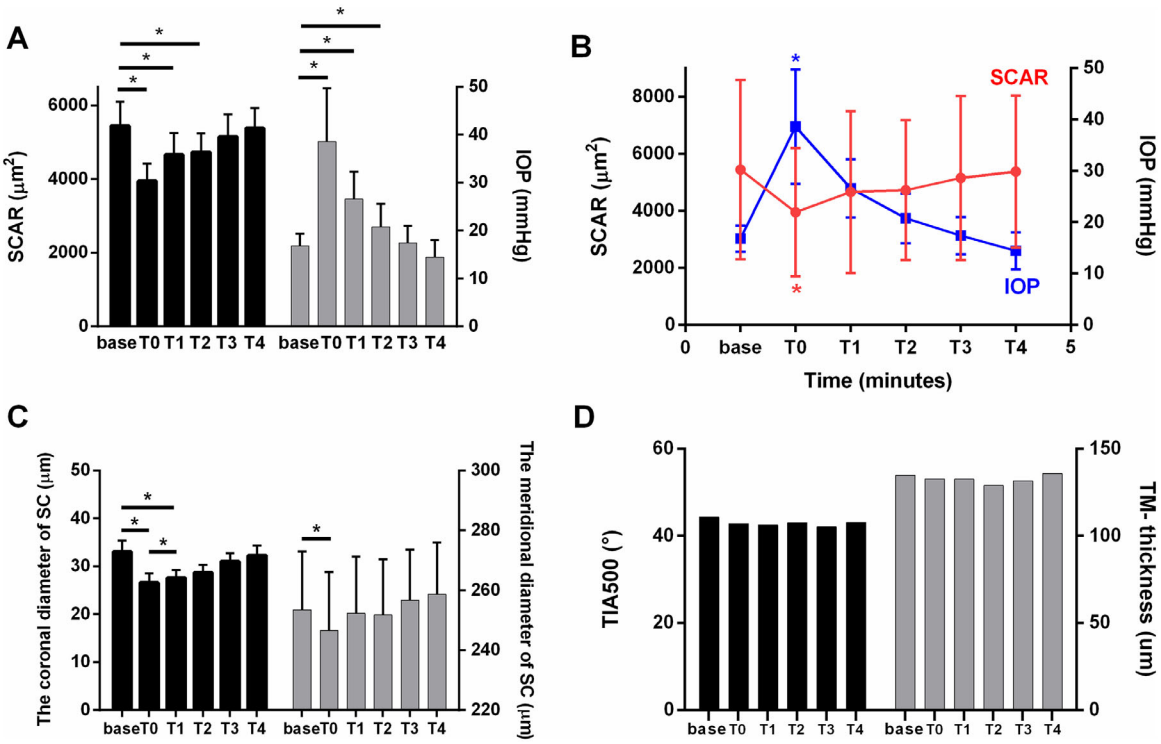

Figure 5. **A,** Histogram of the SCAR and IOP at the different time-points. SCAR decreased significantly at T0 and then returned to baseline at T4; IOP increased, as expected, at T0 and returned to baseline at T4. The black bars depict the SCAR and the gray bars depict the IOP. **B,** The line chart of SCAR and IOP at different timepoints. There was a significant correlation between the SCAR and IOP. **C,** Histogram of the coronal and meridional diameter of SC at different time-points. Both of the coronal and the meridional diameter of SC decreased significantly at T0. The black bars depict the coronal diameter of SC and the gray bars depict the meridional diameter of SC. **D,** There were no significant variations of TM-thickness and TIA500 at different stages. The *black bars* depict the TIA500, and the *gray bars* depict the TM-thickness. Asterisk (*) denotes statistically significant differences (One-way repeated-measures analysis of variance).

with the outflow facility coefficient. Thus, reduction in SC area accounts for the decrease in the outflow facility in the healthy subjects in vivo.

During the examination process, the tonometer applies a constant force to the eye, elevating the IOP. As the IOP decays back to a steady-state, the rate of decay is calculated to determine the outflow facility. The principle is mainly based on the Goldmann equation[30] and measures the rate of IOP drop to plateau levels over about 4 minutes, as follows:

$$F = (P - P_e) \times C - F_u,$$

where F is the aqueous humor flow rate, P is the intraocular pressure, P_e is the episcleral venous pressure, C is the outflow facility coefficient, and F_u is the outflow rate through the unconventional pathway. In our study, C was measured at a wide range of IOPs, based on this principle. We found that C strongly depended on the IOP and the exponential one-phase decay curve best-fit dependence of C and IOP ($R^2 = 0.945$). The result is similar to that reported by Karyotakis et al.,[10] who found a non-linear correlation of C and different IOP levels by using an invasive pump connected with a pressure transducer prior to the cataract surgery.

Reducing IOP is the only evidence-based treatment for glaucoma disease.[31] Several treatments are expected to target the outflow facility to modulate IOP. For instance, breathing nitric oxide has been used to reduce IOP and increase the outflow facility.[32] Tissue plasminogen activator has also used to modulate the outflow facility and control IOP.[33] After phacoemulsification cataract surgery, Alaghband et al.[34] found that the C value improved from 0.14 ± 0.07 before surgery to 0.18 ± 0.09 μL/min mm Hg, which was accompanied by a decrease in the IOP from 15.9 ± 3.66 mm Hg to 13.9 ± 2.9 mm Hg. After timolol treatment, the authors observed that the eye with a higher outflow facility had a larger posttreatment decrease in the outflow facility to achieve a stable IOP level.[35] Various explanations have been proposed for the mechanism by which outflow facility may modulate IOP and retain a stable pressure. Stamer et al.[36] hypothesized that the outflow resistance within the conventional outflow pathway is constantly adjusted in response to the cell stretch caused by the fluctuating IOP; the mechanism might involve extracellular matrix turnover but would require hours and up to several days.[37] However, in our study, the C value did not increase but rather rapidly and continuously declined with an IOP above 20 mm Hg. We considered that the acute pressure increases directly affected the traditional outflow pathway by causing a collapse of SC within the short time-frame of a few minutes. In addition to the decreased SCAR, the coronal diameter of SC but not the trabecular meshwork thickness was found to have decreased markedly, and it seemed that the trabecular meshwork migration into the SC had not occurred. After instillation of tropicamide (to suppress smooth muscle activity), Kagemann et al.[16] found that the SCAR reduced from 4597 ± 2503 μm² to 3588 ± 1198 μm², and the SC inner-to-outer wall distance decreased from 2.34 μm to 0.18 μm

Investigative Ophthalmology & Visual Science

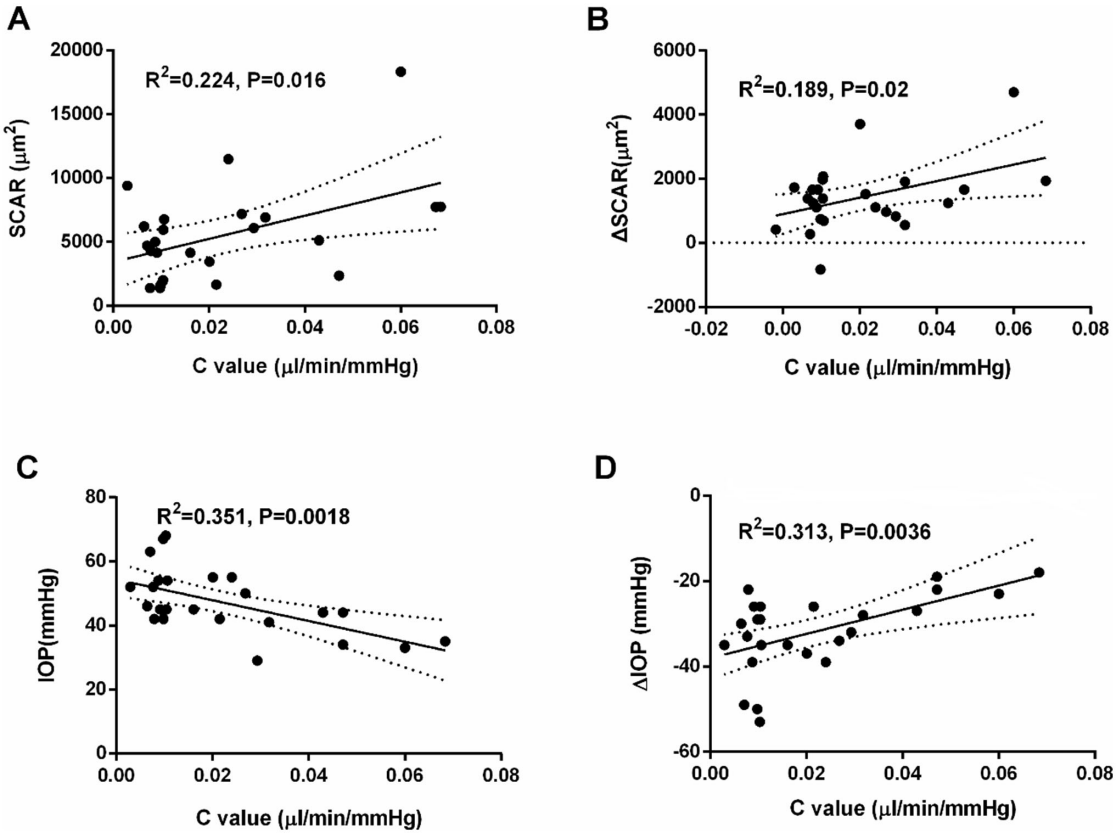

Figure 6. **A,** There was a significant correlation of C_0 and SCAR ($R^2 = 0.224$; $P = 0.016$); **B,** There was a significant correlation of C_0 and ΔSCAR ($R^2 = 0.189$; $P = 0.02$); **C,** There was a significant correlation of C_0 and IOP ($R^2 = 0.351$; $P = 0.0018$); **D,** There was a significant correlation of C_0 and ΔIOP ($R^2 = 0.313$; $P = 0.0036$).

during the similar constant increase in the acute IOP (6 mm Hg). This implies that a control system maintains the SC patency. This should be investigated further in future.

There are a few limitations to our study. First, only young healthy subjects were enrolled. Further research is required to identify whether these changes also occur in elderly people and glaucoma patients. Second, both the nasal and temporal regions were adopted in most of the previous studies. After consideration of the tolerance of subjects and the distortion of the temporal limbus, only one quadrant (nasal side) was chosen. TIA500 of the nasal point was calculated, and it was found to be slightly decreased at T0, but there were no significant differences from the baseline to T4, which implies the stable structure of the anterior chamber in the nasal region. In our previous study, we observed that SC lumen tends to open circumferentially in normal individuals by EDI-OCT.[38] Further research is required to determine the correlation of circumferential of SC and the outflow facility using advanced equipment and methods.

In conclusion, we used OPT to calculate the ocular parameters at the same time as measuring the outflow facility, which has not been reported previously. We found that the dimensions of SC changed in response to the IOP-dependent mechanical force and that these changes appeared to directly affect outflow facility. This study provides insight into the mechanism of outflow facility impedance and can form the basis for further research.

Acknowledgments

The authors thank Yan Xiang and Chaohua Deng for their support in this study.

Supported by the Natural Science Foundation of China (NO: 81974133).

Disclosure: **W. Chen,** None; **T. Hu,** None; **Q. Xu,** None; **Z. Chen,** None; **H. Zhang,** None; **J. Wang,** None

References

1. Goel M, Picciani RG, Lee RK, Bhattacharya SK. Aqueous humor dynamics: a review. *Open Ophthalmol J*. 2010;4:52–59.
2. Carreonab T, der Merwec E, Fellman RL. Aqueous outflow—a continuum from trabecular meshwork to episcleral veins. *Progr Retinal Eye Res*. 2017;57:108–133.
3. Hu Y, Barron AO, Gindina S, et al. Investigations on the role of the fibrinolytic pathway on outflow facility regulation. *Invest Ophthalmol Vis Sci*. 2019;60:1571–1580.
4. Wen JC, Reina-Torres E, Sherwood JM, et al. Intravitreal anti-VEGF injections reduce aqueous outflow facility in patients with neovascular age-related macular degeneration. *Invest Ophthalmol Vis Sci*. 2017;58:1893–1898.
5. Cameron D, Finlay ET, Jackson CR. Tonometry and tonography in the diagnosis of chronic simple glaucoma. *Br J Ophthalmol*. 1971;55:738–741.

6. Grant WM. Tonographic method for measuring the facility and rate of aqueous flow in human eyes. *Arch Ophthalmol*. 1950;44:204–214.
7. Langham ME, Leydhecker W, Krieglstein G, Waller W. Pneumatonographic studies on normal and glaucomatus eyes. *Adv Ophthalmol*. 1976;32:108–133.
8. Torres ER, Wen JC, Liu KC, et al. VEGF as a paracrine regulator of conventional outflow facility. *Invest Ophthalmol Vis Sci*. 2017;58:1899–1908.
9. Johnson M. What controls aqueous humour outflow resistance? *Exp Eye Res*. 2006;82:545–557.
10. Karyotakis NG, Ginis HS, Dastiridou AI, et al. Manometric measurement of the outflow facility in the living human eye and its dependence on intraocular pressure. *Acta Ophthalmologica*. 2015;93:e343–e348.
11. Chen W, Chen L, Chen Z, et al. Influence of the water-drinking test on intraocular pressure, Schlemm's canal, and autonomic nervous system activity. *Invest Ophthalmol Vis Sci*. 2018;59:3232–3238.
12. Yan X, Li M, Chen Z, et al. Schlemm's canal and trabecular meshwork in eyes with primary open angle glaucoma: a comparative study using high-frequency ultrasound biomicroscopy. *PLoS ONE*. 2016;11:e0145824.
13. Römkens HC, Beckers HJ, Schouten JS, Berendschot TT, Webers CA. Reference values for anterior chamber morphometrics with swept-source optical coherence tomography in a Caucasian population. *Clinical Ophthalmology*. 2018;12:411–417.
14. Ulrich WD, Ulrich C, Neunhôffer E, Fuhrmann P. Okulo-Pressions-Tonometrie (OPT)- ein neues tonographisches Verfahren zur Glaukomdiagnostik. *Kim Mbl Augenheilk*. 1987;190:109–113.
15. Stodtmeister R, Pilimat LF, Brenner F. Beurteilung der Kammerwasserdynamik mit der Okulopressionstonometrie nach Ulrich. *Ophthalmologies*. 1988;196:57–66.
16. Kagemann L, Wang B, Wollstein G. Trabecular meshwork response to pressure elevation in the living human eye. *J Visualized Exp*. 2015;100:1–5.
17. Tun TA, Atalay E, Baskaran M, et al. Association of functional loss with the biomechanical response of the optic nerve head to acute transient intraocular pressure elevations. *JAMA Ophthalmol*. 2018;136:184–192.
18. Elsheikh A, McMonnies CW, Whitford C, Boneham GC. In vivo study of corneal responses to increased intraocular pressure loading. *Eye Vis*. 2015;2:1–10.
19. Iwase T, Akahori T, Yamamoto K, Ra E, Terasaki H. Evaluation of optic nerve head blood flow in response to increase of intraocular pressure. *Sci Rep*. 2018;8:17235.
20. Akahori T, Iwase T, Yamamoto K, Ra E, Terasaki H. Changes in choroidal blood flow and morphology in response to increase in intraocular pressure. *Invest Ophthalmol Vis Sci*. 2017;58:5076–5085.
21. Ethier CR. The inner wall of Schlemm's canal. *Exp Eye Res*. 2002;74:161–172.
22. Johnson M. What controls aqueous hµmour resistance? *Exp Eye Res*. 2006;82:545–557.
23. Gong H, Ruberti J, Overby D, et al. A new view of the human trabecular meshwork using quick-freeze, deep-etch electron microscopy. *Exp Eye Res*. 2002;75:347–358.
24. Ten Hulzen RD, Johnson DH. Effect of fixation pressure on juxtacanalicular tissue and Schlemm's canal. *Invest Ophthalmol Vis Sci*. 1996;37:114–124.
25. Murphy CG, Johnson M, Alvarado JA. Juxtacanalicular tissue in pigmentary and primary open angle glaucoma. The hydrodynamic role of pigment and other constituents. *Arch Ophthalmol*. 1992;110:1779–1785.
26. Seiler T, Wollensak J. The resistance of the trabecular meshwork to aqueous humour outflow. *Graefes Arch Clin Exp Ophthalmol*. 1985;223:88–91.
27. Ethier CR, Kamm RD, Palaszewski BA, et al. Calculations of flow resistance in the juxtacanalicular meshwork. *Invest Ophthalmol Vis Sci*. 1986;27:1741–1750.
28. Johnson M, Shapiro A, Ethier CR, Kamm RD. Modulation of outflow resistance by the pores of the inner wall endotheliµm. *Invest Ophthalmol Vis Sci*. 1992;33:1670–1675.
29. Yuan F, Schieber AT, Camras LJ, Harasymowycz PJ, Allingham RR. Mathematical modeling of outflow facility increase with trabecular meshwork bypass and Schlemm canal dilation. *J Glaucoma*. 2016;25:355–364.
30. Allingham RR, de Kater AW, Ethier CR. Schlemm's canal and primary open angle glaucoma: correlation between Schlemm's canal dimensions and outflow facility. *Exp Eye Res*. 1996;62:101–109.
31. Grant WM. Tonographic method for measuring the facility and rate of aqueous flow in human eyes. *Arch Ophthalmol*. 1950;44:204–214.
32. Heybani A, Scott R, Samuelson TW, et al. Open-angle glaucoma: burden of illness, current therapies, and the management of nocturnal IOP variation. *Ophthalmol Ther*. 2020;9:1–14.
33. Muenster S, Lieb WS, Fabry G, et al. The ability of nitric oxide to lower intraocular pressure is dependent on guanylyl cyclase. *Invest Ophthalmol Vis Sci*. 2017;58:4826–4835.
34. Alaghband P, Beltran-Agulló L, Galvis EA, et al. Effect of phacoemulsification on facility of outflow. *Br J Ophthalmol*. 2018;102:1520–1526.
35. Kazemi A, McLaren JW, Trese MGJ, et al. Effect of timolol on aqueous humor outflow facility in healthy human eyes. *Am J Ophthalmol*. 2019;202:126–132.
36. Stamer WD, Acott TS. Current understanding of conventional outflow dysfunction in glaucoma. *Curr Opin Ophthalmol*. 2012;23:135–143.
37. Keller K, Aga M, Bradley JM, et al. Extracellular matrix turnover and outflow resistance. *Exp Eye Res*. 2009;88:676–682.
38. Jing S, Chen Z, Chen W, et al. The 360° circumferential opening of Schlemm' s canal in normal individuals detected by enhanced depth imaging optical coherence tomography. *Medicine*. 2020;99:7(e19187).

Investigative Ophthalmology & Visual Science